Journal of Bioenergetics and Biomembranes, Vol. 30, No. 1, 1998

Determination and Novel Features of the Absolute Absorption Spectra of the Heme *a* Moieties in Cytochrome *c* Oxidase

Yutaka Orii

Received September 16, 1997; accepted September 22, 1997

The absolute absorption spectra of the two heme *a* moieties in cytochrome *c* oxidase were determined in the Soret region where spectral contributions from copper ions are negligible. This determination employs a set of absorption spectra of the enzyme recorded during anaerobic reduction with sodium dithionite, and does not require any other spectral data. The unique feature of the component spectra revealed in the present study suggests the existence of a specific interaction of heme *a* with the immediate environment as its origin. The usefulness of the absolute spectra in quantitative analysis of the spectral data is presented.

INTRODUCTION

Cytochrome *c* oxidase (CCO)[2] is the terminal oxidase of the respiratory chain embedded in the mitochondrial inner membrane and catalyzes the reduction of molecular oxygen into water, pumping out protons from the matrix of mitochondria to the cytosolic side (Babcock and Wikström, 1992). The mammalian enzyme consisting of 13 subunits has two molecules of heme *a*, three copper ions, and zinc and magnesium ions (Kadenbach and Merle, 1981; Einarsdóttir and Caughey, 1984; Bombelka *et al.*, 1986; Steffens *et al.*, 1987). Their location and ligand binding status have been determined by X-ray crystallographic studies on both mammalian and bacterial enzymes (Iwata *et al.*, 1995; Tsukihara *et al.*, 1995,1996). The two heme *a* moieties have different spectral and functional properties that were assigned originally to cytochrome *a* and cytochrome a_3 by Keilin and Hartree (1939). They assumed that cytochrome a_3 was autoxidizable and reacted with respiratory inhibitors like cyanide, carbon monoxide, and others whereas cytochrome *a* did not. The three-dimensional structure indicates the existence of five-coordinate heme *a* with one imidazole axial ligand, and this should react with dioxygen as well as the respiratory inhibitor. The other heme *a* is six-coordinated with two axial imidazole ligands, unreactive toward extrinsic ligands but accepts electron from Cu_A. Hereafter five-coordinate heme *a* that often appears as heme a_3 in the literature will be designated as heme a_B or simply Fe_B and six-coordinate heme *a* as heme a_A or Fe_A for convenience (Miki and Orii, 1986).

Exact knowledge of the absorption spectrum of each heme component in CCO is essential in quantitative analysis of the spectral changes during catalytic turnover as well as in equilibrium studies. Following the proposal by Keilin and Hartree several attempts were made to isolate overlapped absorption spectra of the two heme *a* moieties utilizing their different reactivities with respiratory inhibitors as well as reductants (see Lemberg and Barrett, 1973). However, the absolute absorption spectra so far proposed are not suitable for use in quantitative analysis because of some ambiguity inherent in the derivation procedures. Here, I report a straightforward determination of the absolute absorption spectra of the heme moieties with minimal and reasonable assumptions. The procedure

[1] Department of Public Health, Graduate School of Medicine, Kyoto University, Kyoto 606, Japan.

[2] Abbreviations used: CCO, cytochrome *c* oxidase; *fa*, fractional reduction of Fe_A; *fb*, fractional reduction of Fe_B.

0145-479X/98/0200-0047$15.00/0

employs stopped-flow rapid-scan spectrophotometry to differentiate the two heme *a* moieties both kinetically and spectrally during the anaerobic reduction of the mammalian enzyme with sodium dithionite; heme a_A is reduced first, followed by heme a_B (Yonetani, 1960; Lemberg and Mansley, 1966; Jones *et al.*, 1983; Brunori *et al.*, 1985; Bickar *et al.*, 1986; Nicholls and Wrigglesworth, 1988; Liao and Palmer, 1996). The absolute spectra show several novel features and have quantitatively reproduced the experimental results, thus demonstrating their potential usefulness in the spectral analysis.

EXPERIMENTAL

Materials

Cytochrome *c* oxidase was purified from bovine heart muscle according to the procedure described previously (Orii *et al.*, 1977; Orii, 1984) with a slight modification. The final enzyme preparation was dissolved in 50 mM phosphate buffer, pH 7.4, containing 2% (w/v) sodium cholate, and stored in liquid nitrogen until used. Sample solutions were prepared by dilution with 50 mM phosphate buffer, pH 7.4, containing 0.25% (w/v) polyoxyethylene 2,3-lauryl ether (Brij 35). The concentration of CCO was determined spectrophotometrically by using $\epsilon_{mM} = 33.0$ for an absorbance difference between 605 and 630 nm of the reduced enzyme (Orii *et al.*, 1977).

Stopped-Flow and Rapid-Scanning Spectrophotometry

A stopped-flow rapid-scanning spectrophotometer was designed for handling of anaerobic samples (Orii, 1993), and was used to record spectral changes of CCO during anaerobic reduction with sodium dithionite. Usually a solution in the reservoir was bubbled with oxygen-free nitrogen gas (99.99999%, Teisan) for at least 15 min, followed by flushing of the gas over the surface of the solution. One of the reservoirs contained a solution of CCO and the other 12 mM sodium dithionite (Lambeth and Palmer, 1973; Orii and Anni, 1990). The reaction was initiated by mixing the two solutions at 20°C, and data was collected along the preset logarithmic time axis from 1 ms to 1800 s and stored in a data matrix of 512 × 512. The stored data were retrieved and processed on a desktop computer (Dell OptiPlex XMT 5133 or GXi) by using Matlab (The Mathworks, South Natick, Massachusetts).

RESULTS AND DISCUSSION

Absorption Spectra of CCO in Four Different Redox States

CCO can assume at least four different redox states with respect to the heme *a* moieties. These four states as well as the corresponding absorption spectra will be designated as AOBO, ARBO, AOBR, and ARBR. AOBO signifies that both Fe_A and Fe_B are in the oxidized state, ARBO is for reduced Fe_A and oxidized Fe_B, and so on. Figure 1a shows these spectra that were extracted from the recorded absorption spectra during anaerobic reduction of CCO with sodium dithionite.[3] It is known that in the Soret region contribution of copper ions to the absorption is negligible, and is at most less than 2% of the absorbance at 445 nm (Greenwood *et al.*, 1983, 1988; Farrar *et al.*, 1991; Lappalainen *et al.*, 1993; Lappalainen and Saraste, 1994; Von Wachenfeldt *et al.*, 1994; Slutter *et al.*, 1996). Therefore, the observed spectral changes can be ascribed solely to Fe_A and Fe_B, and in fact the spectral change during the dithionite reduction can be reconstructed by an algebraic combination of the four spectra. This result suggests that the absorption spectra of the heme *a* moieties are independent of each other throughout the reduction process. These properties are well taken in the analyses that follow.

Determination of Absolute Absorption Spectra

Among the component spectra shown in Fig. 1a, ARBO is unique because two peaks assignable to BO and AR are well separated, and in fact this was resolved into four Gaussian peaks on a linear baseline (Fig. 1b). Most simply and tentatively, peaks 1 and 2 in the lower wavelengths region were assigned to BO and peaks 3 and 4 to AR. The background was divided into two parts each for AR and BO by using the combined peak

[3] A part of this work was presented by Y.O. at the XIIth International Congress of Biophysics, Amsterdam, 1966. Manuscript in preparation.

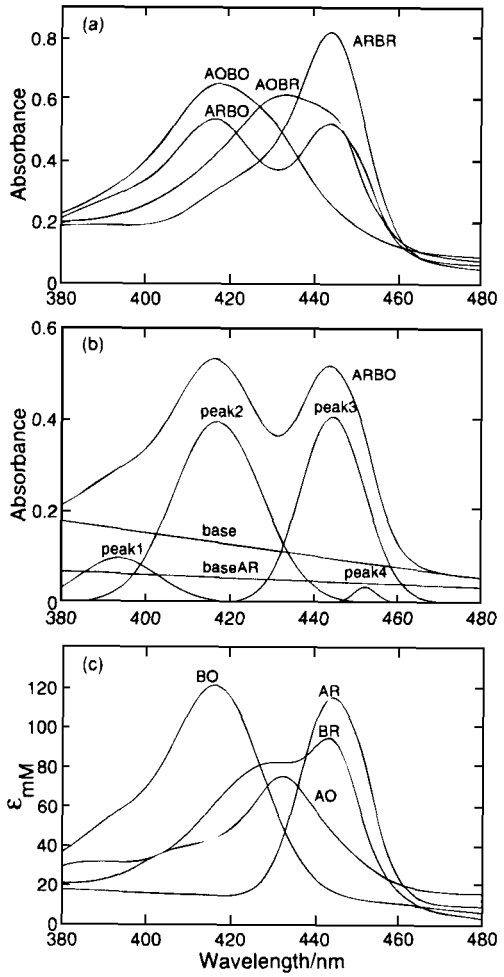

Fig. 1. Spectral analysis. (a) The absorption spectra of CCO (3.92 μM) under four different redox states. The 1001-point spectral data were derived from the original 245-point spectrum (see footnote 3) by interpolation. A designation for each spectrum appears in the text. (b) Resolution of ARBO into Gaussian peaks and a base line. The base line assigned to AR is indicated by baseAR. The ratio of peak area, (peak 1 + peak 2)/(peak 3 + peak 4), is 12.5/8.0. Accordingly, 12.5/(12.5 + 8.0) of the base at 380 nm was allotted to BO (= peak 1 + peak 2), and the same portion at 480 nm to AR (= peak 3 + peak 4) as a trial. (c) The absolute absorption spectra.

area for each species as the weight. Thus AR and BO were determined. The absolute spectra for AO and BR were obtained by subtracting BO from AOBO, and AR from ARBR, respectively (Fig. 1c). It is noted that this derivation requires no other assumption and in principle is done by utilizing only the time-dependent spectral change of a single sample. Consequently there is no experimental ambiguity.

The spectral properties previously shown by Horie (1964) and Vanneste (1966) are summarized in Table I for comparison with the present result. These were derived by using cyanide to suppress the redox change of Fe_B, and carbon monoxide to lock Fe_B in the reduced state. The photochemical action spectrum of the respiratory enzyme determined independently (Warburg and Negelein, 1928) was also employed. The relative peak height of AR to BR is 82.5(441)/213(443) by Horie and 113(444)/125(442.5) by Vanneste. The figures in the parentheses are the peak positions in nm. Although the difference between the two groups is remarkable, they are common in the trend that the relative height of AR/AO is lower than 1 and that of BR/BO higher than 1. The relative height of AR/BR in the present result is 115.1(444.5)/94.7(443.5). This ratio is closer to that of Vanneste though the peak heights are reversed. AR/AO and BR/BO are 1.53 and 0.78, respectively, in contrast to the results given by Horie and Vanneste; these authors reported that AR/AO was lower than 1, and BR/BO higher than 1 (Horie, 1964; Vanneste, 1966). The higher peak of AR than AO derived in the present study is a common property among low-spin *b*- and *c*-type cytochromes.

In the reduced state of CCO, BR is a doublet with major and auxiliary peaks at 443 and 428 nm, respectively (Fig. 1c). This is a novel feature, and entirely different from the absolute absorption spectra so far proposed. These peaks are possibly ascribed to vibrations of the electronic states. An enhanced 0–1 vibration at 428 nm (Gouterman, 1959) may reflect a strong interaction of the excited state with the immediate environment, and an interaction of the heme iron Fe_B with a putative proximal ligand also close to Cu_B, if any,[4] is one of the possibilities. On the other hand, in the oxidized state the AO spectrum is unusually

Table I. Spectral Indices of Heme *a* Moieties in CCO

	AO	AR	BO	BR
Horie (1964)	426[a]	441	412	443
	(88.1)[b]	(82.5)	(113)	(213)
Vanneste (1966)	426	444	414	442.5
	(120)	(113)	(81)	(125)
Present study	432.5	444	416.5	443.5
	(75.0)	(115.1)	(121.2)	(94.7)

[a] Peak positions in nm.
[b] Millimolar extinction coefficient, mM^{-1}, $\cdot cm^{-1}$.

[4] The existence of a corresponding electron density has not been reported explicitly.

broad. It is suggested that Cu_A may contribute to absorption in the Soret region (Tsudzuki *et al.*, 1967; Kobayashi *et al.*, 1989). Although dithionite reduction cannot differentiate kinetically Fe_A from Cu_A due to a rapid electron exchange between them, a pulse radiolysis study has shown that in the early stage of the reduction a preferential absorbance decrease occurs around 410 nm (Kobayashi *et al.*, 1989). Therefore, a small and broad peak recognized around 405 nm may be ascribed to cupric Cu_A although its vibrational origin still remains a possibility. If a discrepancy occurs between the reconstructed and experimental spectral changes for the redox titration around 405 and 444 nm, this result suggests the former possibility.

Second-Derivative Absorption Spectra

The second-derivative absorption spectra of AO, AR, BO, and BR were obtained by numerical calculation as shown in Fig. 2a. In line with the position and number of the component Gaussian peaks, AO shows the bands at 405.0 and 432.4 nm, AR at 443.7 and 451.4 nm, BO at 390.3 and 417.6 nm, and BR at 426.8 and 445.4 nm. With AR the 443.7- and 451.4-nm bands are well separated. Copeland and his associates have proposed that "ferrous cytochrome *a* can adopt two distinct conformations." This proposal is based on their observation that the second-derivative absorption band at 450 nm, assignable to AR, appears when Fe_B is occupied by ligands irrespective of the redox state (Sherman *et al.*, 1991). The present study clearly indicates that the 451-nm band is intrinsic to AR. When the second-derivative operation is applied to the spectrum ARBR the main band appears around 445 nm accompanying a small bump at 450 nm (data not shown). This is an outcome of superposition of the second-derivative bands of AR and BR. Thus it is considered that liganding of CO to BR shifts the second-derivative band of BR to lower wavelengths, revealing the 451- and 444-nm bands of AR. The same argument can be directed to a proposal that "cytochrome *a*" undergoes conformational transition in the steady state of a catalytic turnover because this proposal was also made based on the appearance of the 450-nm band (Copeland, 1991).

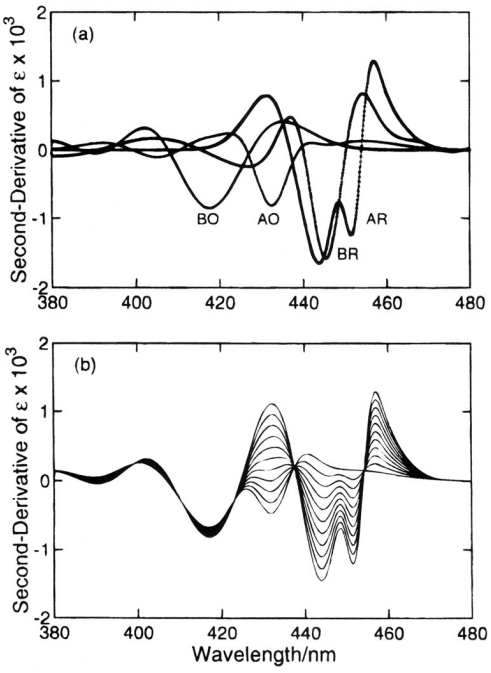

Fig. 2. The second-derivative absorption spectra. (a) The spectra were obtained from the component spectra in Fig. 1c by numerical calculation using Matlab. (b) Initially the simulations of spectral changes for transition from AOBO to ARBO were made; starting from AOBO, AR was increased stepwise (0.1-fraction at a time) while BO was kept unchanged. Then the numerical calculations were applied to obtain the second-derivative spectra. The 443- and 451-nm bands grew as AR increased.

By using the spectra of BO, AO, and AR, I synthesized a series of absorption spectra in which the reduction of Fe_A is assumed to proceed by a 0.1 fraction while Fe_B stays in the oxidized state. Figure 2b shows the second-derivative absorption spectra derived from the synthesized ones, indicating that even when 10% of Fe_A is in the reduced state both 444- and 451-nm bands are apparent as long as Fe_B is in the oxidized state. Thus, in my opinion, the 451-nm is intrinsic to AR and must exist independently of the liganding and redox status of Fe_B. Removal of a mask covering this band will reveal the band. If the origin of the 451-nm band is to be ascribed to strong hydrogen bonding of the Fe_A formyl oxygen to a nearby proton-donating amino acid side chain (Callahan and Babcock, 1983; Sherman *et al.*, 1991), this situation will persist independently of the liganding and redox status of Fe_B, too.

Simulation of Potentiometric Titration

The midpoint potential is not only a fundamental thermodynamic parameter but also essential in estimating the rate of electron transfer between a pair of redox centers (Marcus and Sutin, 1985; Cowan *et al.*, 1988; Beratan *et al.*, 1992; Moser *et al.*, 1992). The experi-

mental determination of the midpoint potential of CCO, however, has been hampered by some inherent technical difficulties mostly due to sluggish attainment of redox equilibrium. To design the experiment it is absolutely necessary to have preliminary knowledge of the time needed for the system to come to equilibrium upon perturbation. This can be accomplished by calculation using the necessary kinetic parameters, but this is seldom done. Also a lack of reliable spectral data of the components that constitute the spectral change inevitably renders the analysis ambiguous. Unless these problems are solved, the analysis is apt to lead to erroneous conclusions. Pertinent discussions and warnings related to this issue have been made previously (Malmström, 1974; Wikström *et al.*, 1981; Hendler and Westerhoff, 1992; Moody, 1996).

Figure 3 shows the simulated spectral changes of CCO for direct potentiometric titrations that will serve as references. In the simulation it is assumed that (1) there is no potentiometric interaction at all among the redox components, (2) copper ions contribute negligibly to the absorbance in the Soret region, and (3) the component absorption spectrum, AO, AR, BO, or BR, is independent of each other. In the initial case the midpoint potential of Fe_A was assumed to be 340 mV (Hendler *et al.*, 1986; Reddy *et al.*, 1986), higher than 234 mV for Fe_B by 106 mV, in accordance with my previous analysis of the reduction kinetics of CCO (see footnote 3). This assignment is contrary to most of the textbook description in biochemistry that quotes the midpoint potential of Fe_B as being higher than that of Fe_A. However, the present assignment is not necessarily new and have some precedents (Bickar *et al.*, 1986; Hendler and Westerhoff, 1992; Snyder, 1992; Moody, 1996). The reduction of Fe_A prior to Fe_B is thus favorable thermodynamically, and is in conformity with the geometric arrangement of the redox components in CCO. The three-dimensional structure of mammalian CCO indicates that the distance between Cu_A, which is assumed to be the site of electron entry to the enzyme, and Fe_A is 20.6 Å compared with 23.2 Å between Cu_A and Fe_B (Tsukihara *et al.*, 1996). This geometry favors the initial reduction of Fe_A (cf. Regan *et al.*, this volume). The simulated spectral change in this case (Fig. 3a) is quite similar to the change that occurs upon anaerobic reduction of CCO with dithionite, and has been observed on several occasions. Initially Fe_A is reduced, followed by reduction of Fe_B, each transition exhibiting the isosbestic point at 436 and 427 nm, respectively. When the midpoint potentials of Fe_A and Fe_B are assumed to be the same at

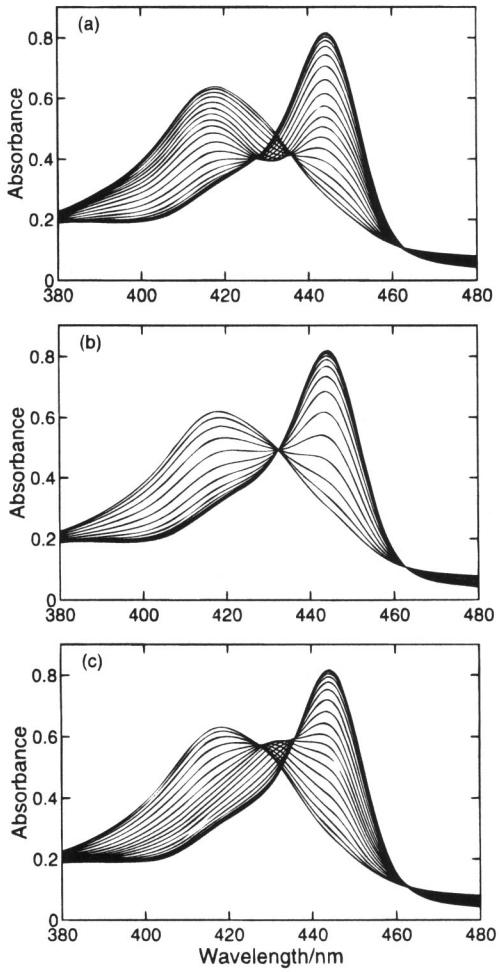

Fig. 3. Simulations of spectral change during the direct potentiometric titration under different conditions. The spectral change was reconstructed from AO, AR, BO, and BR. Both Fe_A and Fe_B were assumed to undergo reduction independently of each other. The midpoint potentials assumed for Fe_A and Fe_B are (a) 340 and 234 mV, (b) 340 and 340 mV, and (c) 234 and 340 mV, respectively. The electrode potential was changed stepwise from 400 to 100 mV in a 5-mV step to induce the absorbance increase at 444 nm. Every third spectrum was presented for clarity.

340 mV, only a single isosbestic point appears at 432 nm throughout the titration (Fig. 3b). If the midpoint potentials assumed in the initial case are reversed, an isosbestic point appears at 427 nm at first and then shifts to 436 nm (Fig. 3c). Thus it is concluded that Fe_A keeps a higher midpoint potential that that of Fe_B throughout the redox transition. If the spectral change registered by the redox or potentiometric titration takes the feature similar to that in Fig. 3b or 3c, we should be cautious to rule out possible involvement of experi-

mental artifacts before being tempted to resort to an alternative interpretation.

Figure 4a illustrates the absorbance changes at 418 and 444 nm versus the electrode potential under three different conditions. The plots represented by circles were derived from the data in Fig. 3a. As the molar absorption coefficients of AO, AR, BO, and BR at every 0.1 nm (Fig. 1c) are available with a known concentration of CCO, the degree of reduction of both Fe_A and Fe_B at varying electrode potentials can be calculated precisely if the absorbances at any two wavelengths are known. The Nernst plots derived give two parallel lines with $n=1$, and are separated by 106 mV (Fig. 4b). As expected, the calculated midpoint potentials of Fe_A and Fe_B are exactly the same as those used in the simulation of the spectral change (Fig. 3a).

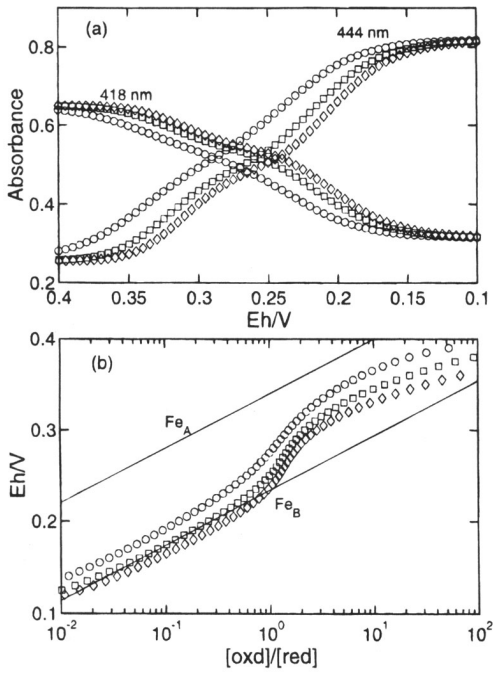

Fig. 4. Analysis of the simulated spectral changes. (a) Simulations of the spectral change were carried out under the same condition as those for Fig. 3a. However, the exponent for fractional reduction of Fe_A, or n for fa^n, was changed from 1 (○) to 2(□) and 3 (◇). From the whole absorption spectra, the absorbance changes at 418 and 444 nm were extracted. (b) The degree of reduction of CCO was calculated from the trace at 444 nm in (a) for each case. The Nernst plots are shown in the corresponding symbols as in (a). The solid lines show the resolution of the traces at 418 and 444 nm in (a) for the normal case (○) in terms of two components. The millimolar extinction coefficients used in the resolution are 45.4, 14.4, 120.3, and 65.3 at 418 nm and 48.3, 114.9, 17.1, and 94.6 at 444 nm for AO, AR, BO, and BR, respectively. The concentration of CCO was 3.92 μM.

When the apparent reduction levels of CCO are calculated based on the absorbance change only at 444 nm, a curve represented by circles is obtained (Fig. 4b). There is a transition around the center of the curve as has been observed experimentally (Wilson and Dutton, 1970), but it does not approach asymptotes with $n=1$ at both the extreme ends. Now, in the reductive potentiometric titration, suppose that a new electrode potential is applied before the current equilibrium is established among the redox centers. This is equivalent to stating that at every electrode potential applied, the reduction of the reducible components is not completed. If *fa* signifies an expected fractional reduction of Fe_A at a specific potential, then fa^2 or fa^3 that is smaller than *fa* is used to simulate the spectral change in place of *fa*. The same operation is applied to *fb*, a fractional reduction of Fe_B. The spectral changes thus derived are the same as for the case with the exponent of 1 in general profiles (Fig. 3a). The corresponding absorbance changes at 418 and 444 nm are shown in Fig. 4a, indicating that the reduction of the heme moieties is retarded accordingly but eventually caught up in a later stage. The apparent reduction level calculated only from the 444-nm trace are shown again for the two cases in Fig. 4b. Deviation from the aymptotes is more apparent. Resolution of a pair of the absorbance changes at 418 and 444 nm in terms of two components yielded two Nernst plots, both being necessarily not straight this time in either case but indicating apparent lowering of the midpoint potential (data not shown). If a similar phenomenon is encountered in the experiment, this is a good sign for incomplete attainment of equilibrium, prompting one to exclude the experimental inadequacy at first.

Thus the absolute absorption spectra of AO, AR, BO, and BR are expected to serve as a powerful tool in analyzing quantitatively as well as qualitatively the numerous spectrophotometric data so far published and yet to come both in equilibrium and kinetic studies. To that end these spectral data will be supplied upon request by e-mail.

ACKNOWLEDGMENTS

This work was supported in part by grants from the Ministry of Education, Science and Culture of Japan and by a research grant from the Fujiwara Foundation of Kyoto University. I would like to thank Dr. T. Kakitani at Nagoya University for discussion.

REFERENCES

Babcock, G. T., and Wikström, M. (1992). *Nature* **356**, 301–309.

Beratan, D. N., Onuchic, J. N., Winkler, J. R., and Gray, H. B. (1992). *Science* **258**, 1740–1741.

Bickar, D., Turrens, J. F., and Lehninger, A. L. (1986). *J. Biol. Chem.* **261**, 14461–14466.

Bombelka, E., Richter, F.-W., Stroh, A., and Kadenback, B. (1986). *Biochem. Biophys. Res. Commun.* **140**, 1007–1014.

Brunori, M., Bickar, D., Bonaventura, J., and Bonaventura, C. (1985). *J. Biol. Chem.* **260**, 7165–7167.

Callahan, P. M., and Babcock, G. T. (1983). *Biochemistry* **22**, 452–461.

Copeland, R. A. (1991). *Proc. Natl. Acad. Sci. USA* **88**, 7281–7283.

Cowan, J. A., Upmacis, R. K., Beratan, D. N., Onuchic, J. N., and Gray, H. B. (1988). *Ann. N.Y. Acad. Sci.* **550**, 68–84.

Einarsdóttir, O., and Caughey, W. S. (1984). *Biochem. Biophys. Res. Commun.* **124**, 836–842.

Farrar, J. A., Thomson, A. J., Cheesman, M. R., Dooley, D. M., and Zumft, W. G. (1991). *FEBS Lett.* **294**, 11–15.

Gouterman, M. (1959). *J. Chem. Phys.* **30**, 1139–1161.

Greenwood, C., Hill, B. C., Barber, D., Eglinton, D. G., and Thomson, A. J. (1983). *Biochem. J.* **215**, 303–316.

Greenwood, C., Thomson, A. J., Barrett, C. P., Peterson, J., George, G. N., Fee, J. A., and Reichardt, J. (1988). *Ann. N.Y. Acad. Sci.* **550**, 47–52.

Hendler, R. W., and Westerhoff, H. V. (1992). *Biophys. J.* **63**, 1586–1604.

Hendler, R. W., Reddy, K. V. S., Shrager, R. I., and Caughey, W. S. (1986). *Biophys. J.* **49**, 717–729.

Horie, S. (1964). *J. Biochem.* **56**, 67–71.

Iwata, S., Ostermeier, C., Ludwig, B., and Michel, H. (1995). *Nature* **376**, 660–669.

Jones, G. D., Jones, M. G., Wilson, M. T., Brunori, M., Colosimo, A., and Sarti, P. (1983). *Biochem. J.* **209**, 175–182.

Kadenbach, B., and Merle, P. (1981). *FEBS Lett.* **135**, 1–11.

Keilin, D., and Hartree, E. F. (1939). *Proc. R. Soc. London* **B127**, 167–191.

Kobayashi, K., Une, H., and Hayashi, K. (1989). *J. Biol. Chem.* **264**, 7976–7980.

Lambeth, D. O., and Palmer, G. (1973). *J. Biol. Chem.* **248**, 6095–6103.

Lappalainen, P., and Saraste, M. (1994). *Biochim. Biophys. Acta Bio-Energetics* **1187**, 222–225.

Lappalainen, P., Aasa, R., Malmström, B. G., and Saraste, M. (1993). *J. Biol. Chem.* **268**, 26416–26421.

Lemberg, R., and Barrett, J. (1973). *Cytochromes*, Academic Press, London and New York.

Lemberg, R., and Mansley, G. E. (1966). *Biochim. Biophys. Acta* **118**, 19–35.

Liao, G. L., and Palmer, G. (1996). *Biochim. Biophys. Acta* **1274**, 109–111.

Malmström, B. G. (1974). *Q. Rev. Biophys.* **6**, 389–431.

Marcus, R. A., and Sutin, N. (1985). *Biochim. Biophys. Acta* **811**, 265–322.

Miki, T., and Orii, Y. (1986). *J. Biochem.* **100**, 735–745.

Moody, A. J. (1996). *Biochim. Biophys. Acta Bio-Energetics* **1276**, 6–20.

Moser, C. C., Keske, J. M., Warncke, K., Farid, R. S., and Dutton, P. L. (1992). *Nature* **355**, 796–802.

Nicholls, P., and Wrigglesworth, J. M. (1988). *Ann. N.Y. Acad. Sci.* **550**, 59–67.

Orii, Y. (1984). *J. Biol. Chem.* **259**, 7187–7190.

Orii, Y. (1993). *Biochemistry* **32**, 11910–11914.

Orii, Y., and Anni, H. (1990). *FEBS Lett.* **267**, 117–120.

Orii, Y., Manabe, M., and Yoneda, M. (1977). *J. Biochem.* **81**, 505–517.

Reddy, K. V. S., Hendler, R. W., and Bunow, B. (1986). *Biophys. J.* **49**, 705–715.

Sherman, D., Kotake, S., Ishibe, N., and Copeland, R. A. (1991). *Proc. Natl. Acad. Sci. USA.* **88**, 4265–4269.

Slutter, C. E., Sanders, D., Wittung, P., Malmström, B. G., Aasa, R., Richards, J. H., Gray, H. B., and Fee, J. A. (1996). *Biochemistry* **35**, 3387–3395.

Snyder, S. H. (1992). *Science* **257**, 494–496.

Steffens, G. C. M., Biewald, R., and Buse, G. (1987). *Eur. J. Biochem.* **164**, 295–300.

Tsudzuki, T., Orii, Y., and Okunuki, K. (1967). *J. Biochem.* **62**, 37–45.

Tsukihara, T., Aoyama, H., Yamashita, E., Tomizaki, T., Yamaguchi, H., Shinzawa-Itoh, K., Nakashima, R., Yaono, R., and Yoshikawa, S. (1995). *Science* **269**, 1069–1074.

Tsukihara, T., Aoyama, H., Yamashita, E., Tomizaki, T., Yamaguchi, H., Shinzawa-Itoh, K., Nakashima, R., Yaono, R., and Yoshikawa, S. (1996). *Science* **272**, 1136–1144.

Vanneste, W. H. (1966). *Biochemistry* **5**, 838–848.

Von Wachenfeldt, C., de Vries, S., and Van der Oost, J. (1994). *FEBS Lett.* **340**, 109–113.

Warburg, O., and Negelein, E. (1928). *Biochem. Z.* **202**, 202–228.

Wikström, M., Krab, K., and Saraste, M. (1981). *Cytochrome Oxidase A Synthesis* Academic Press, London and New York.

Wilson, D. F., and Dutton, P. L. (1970). *Arch. Biochem. Biophys.* **136**, 583–584.

Yonetani, T. (1960). *J. Biol. Chem.* **235**, 845–852.